Flame front surface characteristics in turbulent premixed propane/air combustion

Gulder, O. L.; Smallwood, Gregory J.; Wong, R.; Snelling, D.R.; Smith, R.; Deschamps, B. M.; Sautet, J. -C.

Publisher's version / Version de l'éditeur:

Proceedings of Combustion Institute Canadian Section, 1996 Spring Technical Meeting, pp. 50-1-50-6, 1996

NRC Publications Record / Notice d'Archives des publications de CNRC:
https://nrc-publications.canada.ca/eng/view/object/?id=a3e8911d-5aa5-483f-b31f-4e3106ded269
https://publications-cnrc.canada.ca/fra/voir/objet/?id=a3e8911d-5aa5-483f-b31f-4e3106ded269

FLAME FRONT SURFACE CHARACTERISTICS IN TURBULENT PREMIXED PROPANE/AIR COMBUSTION*

Ö. L. Gülder, G. J. Smallwood, R. Wong, D. R. Snelling, R. Smith, B. M. Deschamps† and J.-C. Sautet‡
National Research Council of Canada, Combustion Research Lab., M-9
Ottawa, Ontario K1A 0R6, Canada

†*Institut Français du Pétrole, 92506 Rueil-Malmaison Cedex, France*

‡*Université de Rouen, Faculté des Sciences - UA CNRS 230 - CORIA*
B.P. 118 76134 Mont Saint Aignan Cedex, France

INTRODUCTION

The attempts to quantify the effects of turbulence on premixed turbulent burning velocity have encountered several challenges, both theoretically and experimentally. The concept of laminar flamelets provides a useful tool to describe the turbulent premixed flames using simple but reasonable assumptions to overcome some of the challenges posed by the problem [1]. This concept assumes that the combustion within a turbulent flame is confined to asymptotically thin moving laminar flamelets which are imbedded in the turbulent flow [1,2]. Since the instantaneous behaviour of these thin layers is the same as those of laminar flames, turbulent burning velocity can be approximated by the product of the flamelets' surface area and laminar burning velocity corrected for the effect of stretch and flame curvature [3]. The two approaches that have been recently used for estimating a measure of the wrinkled flame surface area are the flame surface density concept and the fractal geometry. The flame surface density is defined as the mean flamelet surface area to volume ratio [1].

Fractal dimension, D, of premixed turbulent flames has been measured by several investigators [4-8] and a correlation giving fractal dimension as a function of nondimensional turbulent velocity fluctuation, u'/S_L (ratio of turbulent velocity fluctuation to the laminar burning velocity), has been proposed [7]. This correlation and the experimental data presented in the cited literature assert that the fractal dimension D approaches the fractal dimension of nonreacting turbulent flows 2.37 as u'/S_L increases. Two recent studies [9,10], on the other hand, have been unable to confirm the results of the previous work. The maximum fractal dimension measured (average of several flame images) was 2.21 for u'/S_L =2.4 in a bunsen flame [10] and 2.23 for u'/S_L =8.6 in a V-flame [9]. To resolve this inconsistency, we have carried out an experimental program and determined the fractal parameters of turbulent flames stabilized on two different size Bunsen-type burners. The Reynolds numbers, Re_Λ, based on the integral length scale, Λ, cover the range 40 to 467, and u'/S_L covers the range from 0.9 to 15.

EXPERIMENTAL METHODOLOGY

The turbulent premixed conical flames studied were produced by two axisymmetric Bunsen-type burners with inner nozzle diameters of 11.2 and 22.4 mm. Premixed turbulent propane-air flames with equivalence ratios of 0.8 and 1.0 were stabilized by using an annular propane pilot for low turbulence flames and a hydrogen pilot for high turbulence ones. Turbulence levels were controlled by perforated plates positioned three nozzle diameters upstream of the burner mouth. The turbulence parameters were measured by LDV under reacting conditions where the flow is seeded by fine silicone oil droplets. The length scales, Λ, and turbulence intensities, u', were measured on the burner centerline at the nozzle exit.

The instantaneous flame fronts were visualized by laser induced fluorescence of OH and Mie scattering. A tunable excimer laser (Lambda Physik EMG 150T MSC) was used for both techniques. For planar LIF measurements, the laser was wavelength tuned to a strong OH radical molecular resonance

* *Combustion Institute / Canadian Section, Spring Technical Meeting, May 27-29, 1996, University of Waterloo, Onatrio. Partial funding for the work presented here has been provided by the PERD program.*

line, $Q_1(3)$, which lies within the $A^2\Sigma^+(v' = 0) - X^2\Pi(v'' = 0)$ electronic band. For Mie scattering measurements of the flame front the laser wavelength was set to an off-resonant position within the narrowline tuning range of the laser. The dimensions of the laser sheet at the burner centerline were about 17 cm by 100 μm (FWHM) in the vertical and horizontal planes, respectively. The sheet thickness was less than 150 μm over the full flame width. The sheet optics consisted of a cylindrical lense for vertical plane expansion and a spherical lense for horizontal plane focussing. For LIF of OH, the images were acquired with an intensified CCD detector (Princeton Instruments, 576x384 pixels) giving a flame image spatial resolution of 350 μm. For Mie scattering, the optical detector was a large pixel format CCD detector (Princeton Instruments, 1242x1152 pixels) giving a flame image spatial resolution of 150 μm. Sub-micron oil droplets, generated by a nebulizer, were used as seed material to mark the location of the flame front for the Mie scattering. All LIF and Mie scattering images included full views of the flame.

IMAGE PROCESSING AND ANALYSIS

The ultimate goal of image processing was to produce an image consisting of a line marking the flame front boundary, which was analyzed subsequently using fractal geometry concepts. For both OH and Mie scattering images, the initial step was to remove spurious pixel intensity values by applying a 3X3 median filter. A background image of the flame radiation was then subtracted from each Mie scattering image to improve the signal-to-noise quality of the image. The presence of flame radiation is negligible in OH images since they were acquired at a much shorter exposure time than the Mie images. No attempt was made to correct images for spatial variations in laser intensity. For Mie scattering images, the flame front is marked as a pixel intensity threshold occuring between the unburned and burned gas interface; an interface clearly identified from the extinction (and corresponding loss of optical signal) of the oil droplets as they transit from the unburned to burned gas region. Thresholding an image to a pixel intensity value results in a binary image with dark and light pixels representing, respectively, the burned and unburned gas regions. An edge detection algorithm was then used to obtain a single pixel flame boundary contour.

Compared to Mie scattering images, OH images are more susceptible to spatial variations in the signal-to-noise because of absorption effects resulting from the depletion of the laser sheet intensity as it traverses through the flame, and the self-absorption of the fluorescence signal from OH radicals present between the flame sheet and the detector. OH radicals are present in the burned gas as well as at the flame front. Significant spatial variation of the image signal to noise makes it difficult to assign a single threshold value to mark the flame front position. An improperly chosen threshold value may result in a loss of flame detail in the processed image and subsequently bias the fractal description of the flame. The spatial gradient of the pixel intensity was used to identify the flame front position because the spatial gradient image is relatively insensitive to spatial variations of noise. In the spatial gradient image, pixels along the flame edge have the highest intensities so that the flame edge is clearly distinguishable from other features. A novel algorithm was developed to search for pixels representing local maximum values in the spatial gradient image. These pixels were set to one and all others to zero resulting in a binary image of the flame front contour that effectively preserves the flame detail in the original image.

The caliper method [11] was used for applying the fractal geometry concepts to the flame front images. Although potentially more time consuming, this is a more sensitive measurement than counting methods [12]. A detailed description of the procedure and extraction of the fractal parameters are given in [10].

RESULTS AND DISCUSSION

Fractal Dimension

The fractal dimensions derived from OH and Mie scattering images are almost identical. However, inner and outer cutoffs from OH images are consistently higher than those obtained from Mie scattering images. This may be a reflection of the fact that OH and Mie scattering images indicate slightly different temperature contours within the flame front (OH images indicate a higher temperature con-

tour). The inner cutoffs from OH images are on the average 1.35 times higher than Mie scattering images but for the outer cutoffs this ratio is about 1.12.

Figure 1 shows the fractal dimension data obtained as a function of u'/S_L. A dependence of the fractal dimension on u'/S_L, as reported elsewhere [4,6-8], appears to be nonexistent for the data presented here. The difference between previous measurements and our data is significant for $u'/S_L > 1$. The data of the previous workers [4,6-8] show a fractal dimension about 2.33-2.37 when $u'/S_L \geq 3$. whereas the present work indicates a value about 2.2 for all turbulence intensities considered (Fig.1).

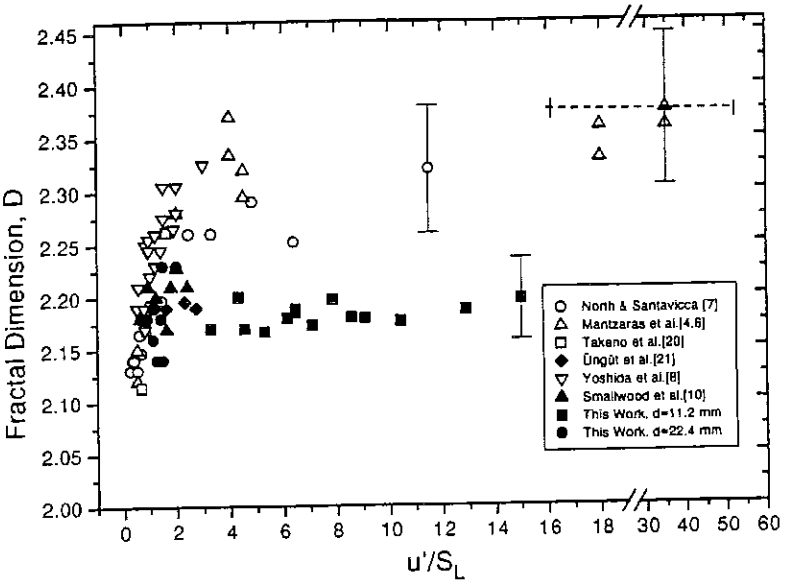

Fig.1. Comparison of the present fractal dimension data to the results of previous studies. For clarity typical error bars are shown for highest turbulence intensity points only. The horizontal error bar of the data point of [4] indicates the range of u'/S_L during the experiment. Please note the axis break and the scale change on x-axis.

How can this discrepancy between the present work and the previous results of the other investigators [4,6-8] be explained ? To address this question, we must first compare the measurement and analysis techniques in each study. A comparison of the measurement techniques showed that the difference in pixel resolutions and laser sheet thicknesses are not large enough to cause the discrepancy observed in Fig.1.

The only remaining distinction between the present work and the previous work of others [4,6-8] is the image analysis method used to extract the fractal parameters. Mantzaras *et al.* [4,6], North and Santavicca [7], and Yoshida *et al.* [8] used the circle method (also called the Minkowski sausage [11]), whereas the caliper method [11] was used in the present study. Although the two methods are equivalent [12] and supposed to yield the same result (on a standard Koch curve, both methods give the value of the theoretical fractal dimension of that curve), to evaluate them a flame image was subjected to both methods. The result of this exercise is shown in Fig.2: The circle method gives a slope of -0.33 whereas the caliper method yields -0.215. For a short range, between about ε =1–2.5 mm, the two methods calculate identical flame lengths, Fig.2. But for larger ε values the calculated flame front lengths differ significantly. Although this observation implicates the image analysis methods used as the cause of the discrepancy in Fig.1, it does not identify which value of the slope corresponds to the correct fractal dimension.

To answer this question, the two methods were applied to an 18 segment quadric Koch island, with the resulting fractal curves shown in Fig.3. The theoretical fractal dimension of this island is 1.6131 [13]. The circle method results in two straight segments on a log-log plot of length versus the measurement scale: neither of the slopes correspond to the correct fractal dimension. With an 8 segment quadric Koch island [13], the circle method produces the correct slope -0.5 for small values of ε, but when ε increases another straight segment is established with a slope of -0.55. For both Koch islands the caliper method gives the correct fractal dimension unambigously. These observations indicate that the caliper technique is a more robust method, and thus that the correct fractal dimension of the flame front surfaces in wrinkled flamelet regime is that reported here, about 2.2.

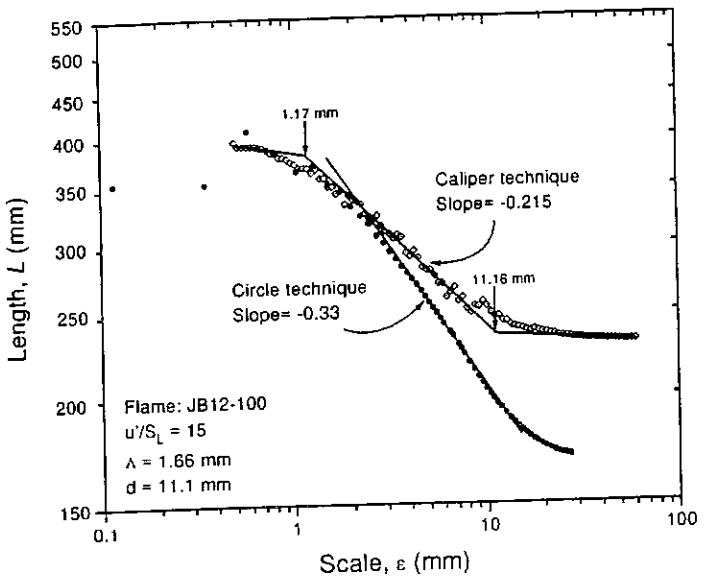

Fig.2. Comparison of the fractal curves obtained by using the circle and caliper methods for one of the flame front images acquired by OH fluorescence.

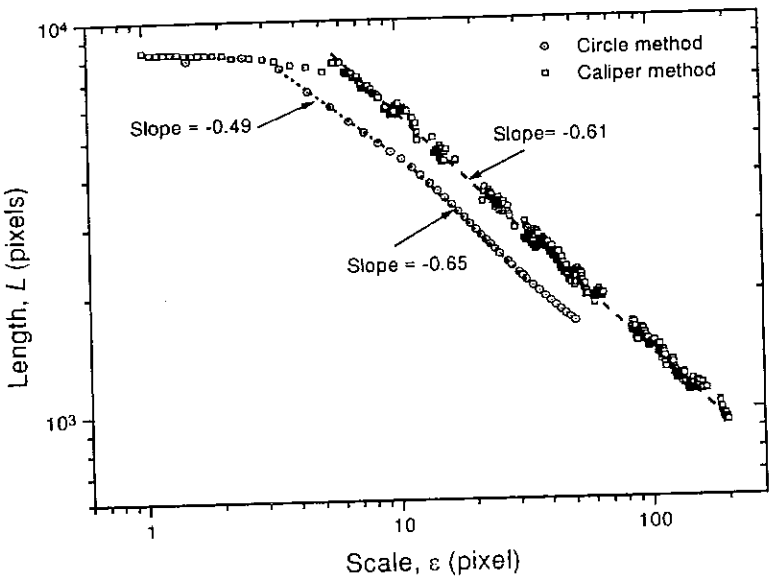

Fig.3. Comparison of the fractal dimension determination by caliper and circle methods on an 18 segment quadric Koch island. The correct theoretical fractal dimension of this island is 1.6131 [13].

Turbulent Burning Velocity

In the laminar flamelet regime the turbulent flame brush consists of thin laminar flames, which are stretched and distorted by turbulence, but retain the internal structure of laminar flames [2]. Within this regime, the mean rate of conversion of reactants into products per unit volume, $< \dot{w} >$, can be expressed as [2]

$$< \dot{w} >= \rho_r S_L^o I_o \Sigma \tag{1}$$

where ρ_r is the density of reactants, I_o is a flamelet stretch and curvature correction term, and Σ is the flamelet surface density. Gouldin *et al.*[14] have proposed a closure model for Σ in terms of fractal parameters for turbulent premixed flames:

$$\Sigma = A(\varepsilon_o/\varepsilon_i)^{D-2} \cdot < c > (1- < c >)/\Lambda_t \tag{2}$$

where A is a model constant, ε_i is the inner cutoff, ε_o is the outer cutoff, $< c >$ is the mean progress variable, and Λ_t is the turbulent flame brush thickness. For conditions where a turbulent flame prop-

agation velocity, S_T, can be defined unambigously, Gouldin[15] showed that

$$S_T/S_L = A(\varepsilon_o/\varepsilon_i)^{D-2} \tag{3}$$

Experimental observations on turbulent premixed flames have shown that $< w >$ (or S_T/S_L) increases with increasing turbulence. So the term $(\varepsilon_o/\varepsilon_i)^{D-2}$ is expected to increase with increasing u'/S_L in accordance with Eqs. 2 and 3. Figure 4 shows the variation of fractal area, $A(\varepsilon_o/\varepsilon_i)^{D-2}$, as function of $(u'/S_L)^{1/2}Re_\Lambda^{1/4}$ assuming A =1. Also shown in Fig.4 is the estimated turbulent burning velocities from reactant flow rates and the cone area of the averaged flame images at $< c >$=0.05. The fractal area shows no evidence of dependence on the approach flow turbulence. The straight dashed line indicates the model proposed by Gülder[16]

$$S_T/S_L = 0.63(u'/S_L)^{1/2}Re_\Lambda^{1/4} \tag{4}$$

which agrees with the estimated S_T/S_L from the reactant flow velocity and the flame cone area.

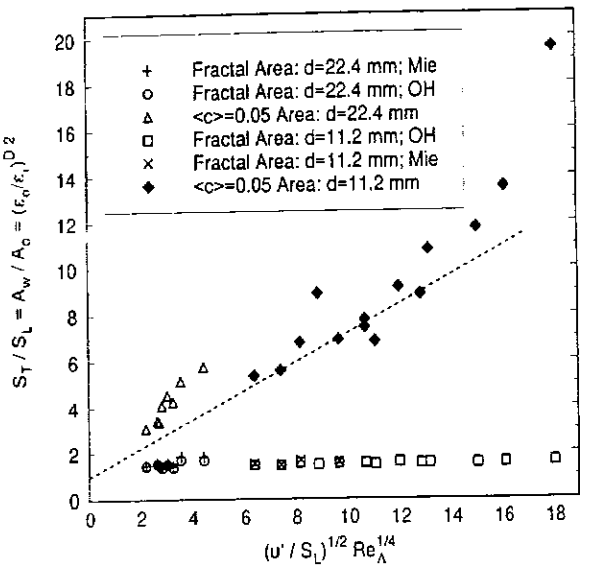

Fig.4. Turbulent burning velocity as determined by fractal and nonfractal methods. For fractal predictions Eq.3 was used. For the nonfractal method, we used the ratio of the area of an equivalent laminar cone ($A_L = Q/S_L$, where Q is the volume flow rate of the premixed reactants) to the area marked by the $< c >$=0.05. The straight dashed line is the prediction of Eq.4.

It was proposed that scales smaller than the laminar flame thickness affect the turbulent flame propagation [17]. It was reported that a proper fractal modelling of turbulent burning velocities should consider both fractal and non-fractal (area increase due to scales smaller than the inner cutoff) contributions [18]. Smallwood *et al* [10], however, has shown that the inclusion of area increase due to wrinkling scales smaller than the inner cutoff has little effect on the fractal prediction of the turbulent burning velocity.

Several turbulent flame propagation formulations, including those based on fractal concepts, are founded on the fundamental assumption that S_T/S_L is proportional to the ratio of the wrinkled flame surface area, A_w, to the flow cross section area, A_o, *i.e.* $S_T/S_L = A_w/A_o$ [19]. If the fractal geometry approach is yielding a true measure of the wrinkled surface area of the flame front, then $S_T/S_L = A_w/A_o$ may not be a reasonable assumption for the turbulent premixed flames in the flamelet regime. Surface density measurements and models may suffer from the same concern. If the area increase (due to increasing turbulence) does not explain the increase in mean burning rate, then it may be proposed that the turbulent transfer of species and heat (enhanced by small scale turbulence) should have a significant role in turbulent premixed combustion. This observation supports the analytical work of Ronney and Yakhot [17] that concludes that the effect of scales smaller than the laminar flame front thickness are probably significant for most flames at sufficiently high turbulence intensities.

Acknowledgements:

The authors thank Y. Côté, T. Zakutney and B. C. Benning for their assistance in the data analysis. We acknowledge the advice given by Professor S. Tavoularis, of University of Ottawa, on turbulence measurements. B. M. Deschamps and J.-C. Sautet were Summit Postdoctoral Fellows at the National Research Council of Canada during this study.

REFERENCES

1. Bray, K. N. C., in *Complex Chemical Reactive Systems* (J. Warnatz and W. Jäger, Eds.), Springer-Verlag, 1987, pp.356-375.
2. Cant, R. S., and Bray, K. N. C., *Twenty-Second Symposium (International) on Combustion*, The Combustion Institute, Pittsburgh, 1987, pp.791-799.
3. Bray, K. N. C., and Cant, R. S., *Proc. R. Soc. Lond.* A 434:217-240 (1991).
4. Mantzaras, J., Felton, P. G., and Bracco, F. V., *SAE Paper No. 881 635*, 1988.
5. Murayama, M., and Takeno, T., *Twenty-Second Symposium (International) on Combustion*, The Combustion Institute, Pittsburgh, 1989, pp.551-559.
6. Mantzaras, J., Felton, P. G., and Bracco, F. V., *Combust. Flame* 77:295-310 (1989).
7. North, G. L., and Santavicca, D. A., *Combust. Sci. Technol.* 72:215-232 (1990).
8. Yoshida, A., Kasahara, M., Tsuji, H., and Yanagisawa, T., *Combust. Sci. Technol.* 103:207-218 (1994).
9. Das, A. K., *Fractal Analysis of Premixed Turbulent Flames*, University of British Columbia, Ph.D. Thesis, 1993.
10. Smallwood, G. J., Gülder, Ö. L., Snelling, D. R., Deschamps, B. M., and Gökalp, I., *Combust. Flame* 101:461-470 (1995).
11. Mandelbrot, B. B., *The Fractal Geometry of Nature*, Freeman, New York, 1982, pp. 25-32.
12. Shepherd, I. G., Cheng, R. K., and Talbot, L., *Exp. Fluids* 13:386-392 (1992).
13. Mandelbrot, B. B., *The Fractal Geometry of Nature*, Freeman, New York, 1982, pp. 50-53.
14. Gouldin, F. C., Bray, K. N. C., and Chen, J.-C., *Combust. Flame* 77:241-259 (1989).
15. Gouldin, F, C., *Combust. Flame* 68:249-266 (1987).
16. Gülder, Ö. L., *Twenty-Third Symposium (International) on Combustion*, The Combustion Institute, Pittsburgh, 1991, pp.743-750.
17. Ronney, P. D., and Yakhot, V., *Combust. Sci. Technol.* 86: 31-43 (1992).
18. Mantzaras, J., *Combust. Sci. Technol.*86: 135-162 (1992).
19. Damköhler, G., *Ze. Elektroch. 46:601-652(1940).* (English Translation NACA TM 1112, 1947.)
20. Takeno, T., Murayama, M., and Tanida, Y., *Exp. Fluids* 10: 61- 70 (1990).
21. Üngüt, A., Gorgeon, A., and Gökalp, I., *Combust. Sci. Technol.*92: 265-290 (1993).

F. Lin

THE
COMBUSTION INSTITUTE
CANADIAN SECTION

1996
SPRING TECHNICAL MEETING
University of Waterloo
Waterloo, Ontario
May 27 - 29

Organized to promote the
science and application
of combustion